AD-A051 301 NAVAL RESEARCH LAB WASHINGTON D C F/G 11/2
FRACTURE INITIATION IN IRDOME GRADE MGF2.(U)
JAN 78 R W RICE, S M MOREY, F W FRASER
UNCLASSIFIED NRL-MR-3685 SBIE-AD-E000 112 NL

| OF |
AD
A051301

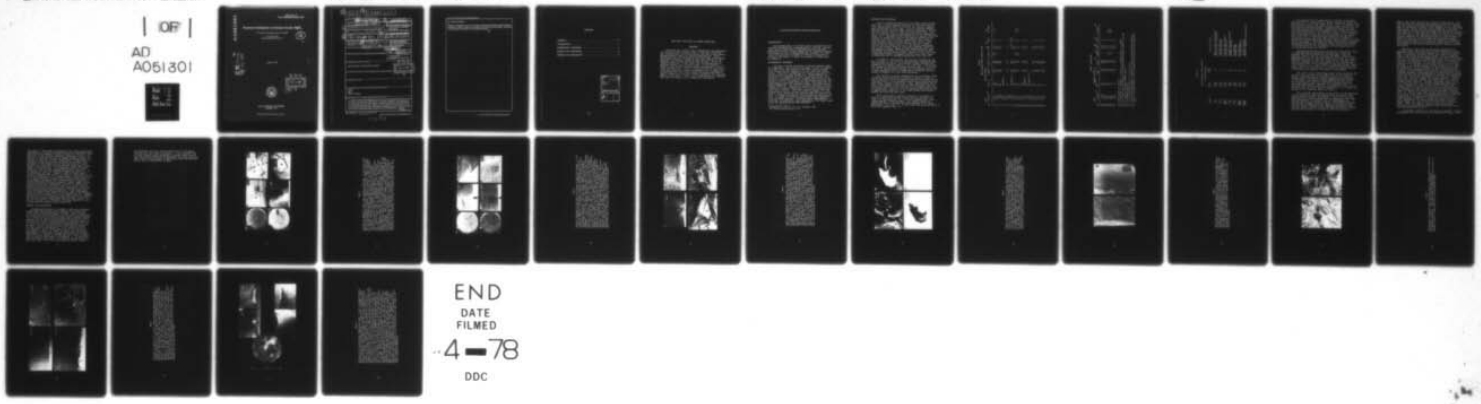

END
DATE
FILMED
4-78
DDC

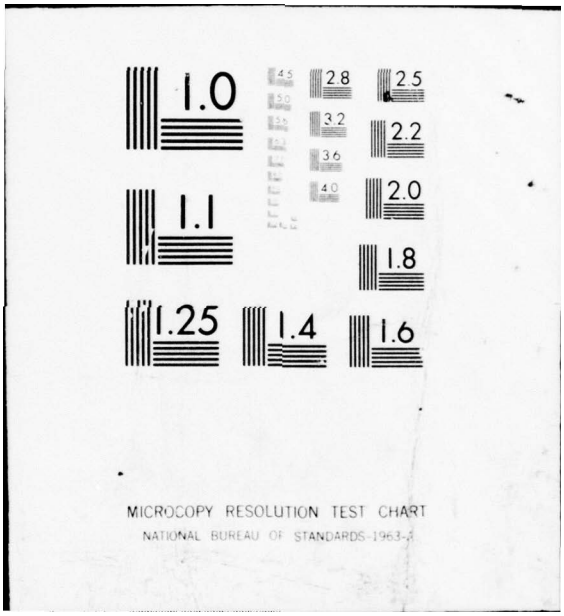
1.0
1.1
1.25
1.4
1.6
1.8
2.0
2.2
2.5
2.8
3.2
3.6
4.0
4.5
5.0
MICROCOPY RESOLUTION TEST CHART
NATIONAL BUREAU OF STANDARDS-1963-A

NRL Memorandum Report 3685

Fracture Initiation in Irdome Grade MgF_2

R. W. RICE, S. M. MOREY and F. W. FRASER

Ceramics Branch
Engineering Materials Division

January 1978

NAVAL RESEARCH LABORATORY
Washington, D.C.

(18) SBIE (19) AD-E000 112

SECURITY CLASSIFICATION OF THIS PAGE (When Data Entered)

REPORT DOCUMENTATION PAGE	READ INSTRUCTIONS BEFORE COMPLETING FORM
1. REPORT NUMBER: NRL Memorandum Report 3685 (NRL-MR-3685) (12) (9)	3. [redacted] Interim rept.
4. TITLE (and Subtitle): FRACTURE INITIATION IN IRDOME GRADE MgF_2 (6)	5. TYPE OF REPORT & PERIOD COVERED: Interim report on a continuing NRL problem.
	6. PERFORMING ORG. REPORT NUMBER
7. AUTHOR(s): R. W. Rice, S. M. Morey, F. W. Fraser (10)	8. [redacted] RR022-02, F54595 (11)
9. PERFORMING ORGANIZATION NAME AND ADDRESS: Naval Research Laboratory, Washington, D. C. 20375 (9) RR022-02-41, WF54595-02	10. PROGRAM ELEMENT, PROJECT, TASK AREA & WORK UNIT NUMBERS: NRL Problem C05-28, PRO2 20241; and C03-26B, WF 54-595-201 and WF54-542-202
11. CONTROLLING OFFICE NAME AND ADDRESS (11)	12. REPORT DATE: Jan[redacted]78
	13. NUMBER OF PAGES: ~~25~~ (13) 30 pp.
14. MONITORING AGENCY NAME & ADDRESS (if different from Controlling Office)	15. SECURITY CLASS. (of this report): UNCLASSIFIED
	15a. DECLASSIFICATION/DOWNGRADING SCHEDULE

16. DISTRIBUTION STATEMENT (of this Report)

Approved for public release; distribution unlimited.

DDC RECEIVED MAR 16 1978 B

17. DISTRIBUTION STATEMENT (of the abstract entered in Block 20, if different from Report)

18. SUPPLEMENTARY NOTES

19. KEY WORDS (Continue on reverse side if necessary and identify by block number)

Irdomes
MgF_2
Fracture processing

20. ABSTRACT (Continue on reverse side if necessary and identify by block number)

Analysis of Irdome grade MgF_2 specimens from one of the leading MgF_2 manufacturers showed that 50-75% often failed from foreign particles or occasionally large grains. The foreign particles were almost exclusively SiO_2, which appears to be introduced by abrasion from the SiO_2 crucibles used for processing the SiO_2 powder. Elimination of these particles would be relatively easy, but is not expected to significantly raise strengths because machining flaws, which are the other predominant source of failure limits strengths to similar levels as the SiO_2 particles do. Practical
(Continues)

DD FORM 1 JAN 73 1473 EDITION OF 1 NOV 65 IS OBSOLETE S/N 0102-014-6601

251950

20. Abstract (Continued)

limitation on reducing the sizes of machining flaws indicate that if significantly improved mechanical performance of Irdomes is required, it is not likely to be obtained by improving MgF_2. Development of new materials is thus required to provide higher performance.

CONTENTS

FOREWORD

This work was carried out in cooperation with personnel of the Naval Weapons Center (NWC), China Lake, primarily Drs. George Hayes and Marian Hills, and one of the leading manufacturers of MgF_2 for optical applications. While materials from only one manufacturer have been investigated and failure analysis focuses on the worst defects in the material, two factors should be kept in mind. First, extensive experience at NWC shows that the manufacturer's material studied are typically equal, if not superior, in terms of both optical and mechanical performance to that of other manufacturers. Second, it must be kept in mind that there are important economic constraints on the production of materials and that these optical materials represent a highly competitive business in which purchases are typically made on a bid basis. Hence, while improvements are desired, they must be achieved on a competitive cost basis.

FRACTURE INITIATION IN IRDOME GRADE MgF_2

INTRODUCTION

Hot pressed MgF_2 is the most widely used material for infrared transmission to approximately 5 microns. Increasingly severe conditions of advanced applications make mechanical failure of MgF_2 components an important problem. The purpose of this investigation was therefore two fold; first to determine the causes of failure, and second to determine the extent to which the strength of MgF_2 might be improved.

EXPERIMENTAL PROCEDURE

Two sets of disks fractured in biaxial flexure tests were examined. The first set of disks, ~ 3.35" in diameter by 0.080" thick were tested at NWC with inner and outer ring loading having diameters of 1.51" and 3.12" respectively. This set of disks was all from one production lot and hence from the same powder lot. The second set of disks 1.25" in diameter by 0.15" thick were tested (with an outer ring support of 0.98" diameter and an inner ring support of 0.35" in diameter) by the manufacturer that was the source of the disks tested at NWC. The second set of disks represented five different powder lots used in processing (Table 2). The area of fracture initiation was determined by visual examination of the crack branching patterns (e.g. Fig. 1, 2). The exact fracture origin was then determined by use of typical fracture markings, i.e. mist hackle, crack branching and fracture steps as described by Rice, (1) using both optical and scanning electron microscopy. A number of fracture origins were also examined by electron probe analysis. Fracture energy measurements were made on samples cut from fragments of the larger disks using the applied moment DCB technique.*

*Measurements made by Dr. S.W. Freiman, NRL

Note: Manuscript submitted December 16, 1977.

RESULTS AND DISCUSSION

Table 1 summarizes results of the disks tested at NWC. Note that of the 30 samples received for fracture analysis (one tested sample was not received) the fracture origins were determined in 27 of them. In 25 of those 27 samples, specific failure causing flaws could be determined. Of the 25 flaw origins, 15 (i.e. 60%) were particles (Figs. 1-4) and ~ 10 surface flaws as determined by optical examination (Figs. 2,5). Subsequent SEM examination of several fractures (Table I), showed that some of the samples identified as failing from flaws by optical examination were found to actually have failed from particles (Figs. 3A,B). Thus, some irregular particle-flaw combinations that caused failure did not always show up in the optical microscopy due to the limited depth of focus and irregular nature of the fracture origin. Based on this observation the total percentage of samples failing due to the presence of particles may reach as high as 75%. However, it is clear that a measurable number of samples did fail from flaws, some of which are due to polishing operations (e.g. Fig. 5).

In order to corrorborate the fracture analysis of the data in Table 1, the fracture energies were calculated from the measured strengths, the observed failure causing flaw dimension and Young's modulus (~ 16×10^6 psi). The resultant average calculated fractured energies were $4 \pm 1\text{-}2$ J/m^2 for all of the specimens together or any subgroup which is in good agreement with the independently measured fracture energy of samples cut from these specimens.

The results of optical examination of the smaller disks tested by the manufacturer are shown in Table 2. Here it can be seen that of the 14 samples examined 10 clearly failed from particles, 2 from unknown sources and 2 from either surface chips, cracks or particles. Thus, approximately 70% or more of the samples failed from foreign particles, many of which were located in the interior of the sample rather than at the surface. Further, with the possible exception of the 2 samples from Powder Lot 3, all other powder lots showed samples failing from particles.

Of 10 particles at fracture origins of the disks analyzed in an electron probe 7 were found to be SiO_2, e.g. Figs. 1,4 (see also Fig. 7), by direct comparison of x-ray counts against a SiO_2 standard. Two however showed no difference from the matrix and hence appeared to be large MgF_2 grains (e.g. Fig. 3). In one case a particle was found to be a zinc compound (Fig. 2).

Table 1

MgF_2 Polished Disks Tested at NWC

Disk No.	σ_f (ksi)(1)	Fracture Origin Type (2)	a(μm)(3)	b(μm)(4)	d(μmB)	(6) (AZ)	(7) γ^J/m^2	(8) σ_f^1 (ksi)
1	10.8	IP+C	150	150	300	0.6	5	7.8
2	17.9	SC	90	400	-	2.0	7	
3	9.59	SC	90	400	-	2.0	7	
4	9.43	SC	150	150	-	0.8	5	
5	16.6	possibly I						
6	15.2							
7	13.3	SC	30	100	-	1.6	4	
8	9.92							
9	13.6	irregular SC	100	350	-	2.0(9)	16(9)	
10	6.83	P+C	130	130	-	0.8	2	
11	12.1	IP	25	50	50	1.1	3	11.5
12	11.0	IP	50	80	150	1.1	4	9.3
13	11.8	SC						
14	14.8	P+C	50	60	-	0.9	5	
15	13.1	probably P	40	50	-	1.1	4	
16	8.75	SC	50	150	-	1.4	3	
17	12.6	irregular I (P)						
18	16.6	P						
19	13.2	SC	25	150	-	2.0	4	
20	14.3	P	50	40	-	0.8	4	
21	13.7	P	25	110	-	1.8	4	
22	14.1	SC	50	140	-	1.6	7	
23	13.2	P	60	50	-	0.8	4	
24	10.9	P	100	100	-	0.8	4	

Table 1 (Continued)

Disk No.	σ_f (ksi) (1)	Fracture Origin Type (2)	a(μm) (3)	b(μm) (4)	d(μmB) (5)	$(AZ)^{-2}$ (6)	γ^J/m^2 (7)	σ_f^1 (ksi) (8)
25	9.85	SC	25	150	-	2.0	3	
26	11.6	SC	30	300	-	2.0	3	
27	14.6	SC	40	100	-	1.3	4	
28	10.6	IP	20	40	50	1.1	1	10.0
29	12.8	IP	30	60	15	1.1	5	12.5
30	14.5	P	35	40	-	0.8	3	
31	15.2	P	50	50	-	0.8	4	

(1) Surface stress at fracture

(2) P = particle, I = internal, C = crack (e.g. polishing flaw), S = surface

(3) & (4) a and b are the semi axes of the approximate elliptical shape of the flaw

(5) d = depth of flaw below tensile surface

(6) flaw geometric factor

(7) $\gamma = 4.4 \times 10^{-4}(AZ)^{-2}\,\sigma^2 a$, σ in. psi, a in μm

(8) failure stress approximately corrected for depth of failure below the surface

(9) note, if the deeper portion of this irregular flaw acted like a half penny flaw, $\gamma \sim 6$.

Table 2

MgF_2 Polished Disks Tested

by Manufacturer

Spec. #	σ_f (ksi)	Prod. Lot	Fracture Origin
7-1	10.8	1	gouge or chip ~150 μ deep
7-2	14.8	1	large grains or particles
17-1	14.2	1	internal particle
-2	13.2	1	internal particle
22-3	14.3	1	particle near surface
22-4	15.7	1	internal particle
31-1	14.6	2	surface chip (or particle)
-2	8.5	2	internal particle
36-3	6.5	3	not detected
-4	14.2	3	surface flaw
103-1	6.5	4	not detected
103-2	16.0	4	internal particle
105-1	11.6	5	internal particle
105-2	8.0	5	surface - possibly from particle

Discussions with the manufacturer revealed the probable sources of all of these failure causing foreign particles with the exception of the large MgF_2 grains. Thus, for example, the manufacturer reports that coarse finish SiO_2 crucibles are used for calcining the MgF_2 powder. Examining sections of these crucibles supplied by the MgF_2 manufacturer shows that while the interior surface of the crucible is not a likely source of such loose SiO_2 grains, the outside surfaces of the crucibles are an extremely likely source of such grains of the proper size, e.g. Fig. 6. Thus the major source of failures is attributed to SiO_2 particles which are readily abraded off the exterior surface of the SiO_2 crucibles that are used in processing of the powder. Use either of other crucibles or possible subsequent screening of the powder could thus be major steps to the reduction if not elimination of this primary source of foreign particles for failure.

The MgF_2 manufacturer also stated that occasionally some Zn compounds are hot pressed in the same facilities and possibly the same dies are used for the MgF_2. Thus the possible cause of the one Zn containing impurity was a small agglomerate of powder that was either left in the die from a previous pressing, or that fell into the die from some other piece of equipment. Since this appears to be a rather rare occurrence it may not be necessary to take precautions against this. However, if it were to be a significant problem, then separation of the facilities or the dies or greater cleaning of dies would be possible solutions to this problem.

The source of the large MgF_2 grains cannot be determined at this time. Whether or not they occur in the starting powder or whether they may possibly be due to an impurity causing highly localized, extreme exaggerated grain growth is not known. The electron probe analysis did not reveal any obvious local impurity concentration associated with the large MgF_2 grains. However, it is possible that impurities were either beyond the detectability limits or quite possibly that they were fugitive impurities, i.e., driven off during the hot pressing operation itself.

Next consider the question of the effect of the particles on the strength of MgF_2 and improvements in strength that might result from their elimination. Analysis of the most extensive data, Table I, shows that the particles while somewhat detrimental to strength were not overwhelming in determining strength levels of MgF_2. The average strengths for the set of samples failing from the particles and the set not failing from particles (based on the optical examination) shown in Table I were both essentially $12 \pm 2 \times 10^3$ psi and this average is the same as that for specimen in

Table 2 that were dominated by failure from particles. Also, failure from particles are approximately evenly distributed over the range of strengths in both Tables 1 and 2. Although some of the samples in Table 1 that appeared to have machining flaw origin, in fact had particles as sources of failure, consideration of this does not change the results significantly. Also, many of the particles that acted as a source of failure were not right at the specimen surface, but correction of the failure strengths for the actual location of the failure resulted in only very limited lowering of failure stresses. Thus, the particles do not result in significant lowering of the flexural strength of the material, which places the maximum stress on the surface favoring surface flaws as sources of failure.

Because the particles are scattered throughout the material volume, they could have a more significant effect under more uniform tensile stresses, e.g. under true tension. Thus, in practice the effect of the particles will depend some on the actual stress distribution. If the stress gradient in the material is substantially less than in the flexure test then the particles could be more severe in terms of the failure of the samples. On the other hand, if: the stress gradient in actual practice is similar to that of the flexure test, i.e., maximum stress on the surface with it rapidly dropping off in the interior, as some thermal stresses do and 2) the foreign particles are not too serious or detrimental to the strength, then the SiO_2 particles may not be a serious problem. Correspondingly, it should also be recognized that the thicker the sample the greater the probability there is of having the particles act as a source of failure since this typically reduces the stress gradient. This is consistent with more failure from particles in the smaller, thicker disks (Table 2). Further, large MgF_2 bars (.5" x .75" cross section) from the same manufacturer fractured in 3 point flexure (3.5" span) had 3 out of 11 fail from foreign particles despite the fact that the surfaces were not polished, but only ground so they had larger machining flaws to compete with the particles as sources of failure (Fig. 7). On the other hand, as the surface area increases, as in going from a disk to a hemispherical shell or dome, the probability of having a more severe surface flaw, e.g. from finishing, increases. Finishing of such curved surfaces, especially the concave side, may result in more severe flaws, e.g. due to greater difficulty of swarf removal. Thus, for example, the one actual failed dome available for analysis was found to have failed from a surface finishing flaw (Fig. 8).

An important question is the degree of possible strength improvement that can be practically achieved in MgF_2. Since

the effect of particles on strength is not high, significant improvement in strength requires reduction of machining flaws which are the predominant remaining source of failure. The question is then how much strength improvement could be achieved by reducing the size of larger finishing flaws. Reduction in the size of these flaws would of course result in strength increasing since the strength is inversely proportional to the square root of the flaw size. It is not possible to unequivocably determine what percentage of the present flaws are from: (1) incomplete removal of larger flaws left from earlier coarser machining by the final polishing, (2) the final polishing operation itself, or (3) by subsequent handling. However, study of these flaws strongly suggests that several of them are characteristic of flaws from polishing, e.g., compare Figs. 5 and 8 with Fig. 7. It is also important to recall that as the surface area of the component increases then the probability of having a larger machining flaw also increases. Hence, based on this and other extensive observations of flaws in ceramic components and the data in Table 1 and 2, it is felt that it would be difficult and quite likely impractical to increase the average strength much beyond the $\sim$ 10,000-15,000 psi level by improved machining operations. Such improvement would also most likely result in an increase in the standard deviation and the extent of low scattered strengths. However, whether this can be achieved at practical cost is uncertain. The limited strength improvement seen for MgF_2 clearly indicates the need for a different IR window material to meet future expected thermal stress conditions.

SUMMARY AND CONCLUSIONS

Examining fractures of a number of optically polished, irdome grade MgF_2 disks clearly showed that foreign particles were the major source of failure. Most of these particles are SiO_2 which appear to come from the loose grain on the outside of the SiO_2 crucibles used in powder processing. While the effect of the foreign particles on failure depends some on the stress distribution; they had little or no effect on flexure strengths where the maximum stress is on the surface with a significant stress gradient into the material, in part because of their distribution throughout the volume of the material. It is noted that while the removal of these foreign particles is both practical and feasible, that it is likely to result only in limited improvement in strengths. Further, practically achievable improvements in surface finishing are also likely to result only in limited improvement in strengths. It is estimated that strengths of the order of 15,000 psi may be about the practical upper limit for typical MgF_2 IR window or dome

size samples, and even those strengths may be achievable reliably only with great difficulty. It is concluded that if significantly higher strengths of thermal shock resistance are required for such IR materials that these are much more likely to be obtained by developing other IR materials rather than by improvement of MgF_2.

A
10
B
100 µm
F
F
F
C
C
20 µm
F
F
P
C
C
D
12
E
100 µm
P
F
20 µm
P

Figure 1

Failure of MgF_2 test disks from foreign particles. A and D are low magnification photos of failed disks No. 10 (the weakest one) and No. 12 (intermediate strength) listed in Table 1. Note the amount of cracking correspondingly increasing with the failure stresses. The arrows indicate the approximate location of the fracture initiation. B and C are higher magnifications of the actual fracture surface of disk No. 10 showing fracture initiation from the semi-circular flaw, F. propagating out from the central particle, P. Also, note the associated cracks, C, which had they been completed could have led to surface spalling. E and F are higher magnifications of the actual fracture surface of disk No. 12 showing failure from a foreign particle, P, located somewhat inside of the surface. Note the porosity (black dots) indicated along the bottom periphery of the particle in F. Electron probe analysis of this particle showed the particle to be SiO_2. Note that in both figures C and F that the fracture character of the particle is consistent with conchoidal fracture of glasses such as fused SiO_2.

A
14
B
200µm
C
10µm
D
21
E
200µm
F
10µm

Figure 2

Further examples of fracture initiation in MgF_2 test disks. A and D are low magnification photos of failed disks Nos. 14 and 21 listed in Table 1. The arrows indicate the approximate location of failure initiation. Note the greater amount of cracking in these disks consistent with their higher than average failure stresses. B and C are higher magnifications of the actual fracture surface of disk No. 14 showing failure from a foreign particle (P) very near the surface. Note that the orientation of the sample in C is different from that in B. Note also in C that the foreign particle has a number of steps suggestive of crystallographic character consistent with the fact that electron probe analysis showed this to be a Zn rich particle which would be consistent with the crystallographic character to the surface of the particle. E and F are high magnification photos of the actual fracture surface of specimen No. 21 showing failure from a surface flaw which may represent either surface damage, e.g. from localized contact or impact or could possibly represent spallation from a foreign particle which is not exposed.

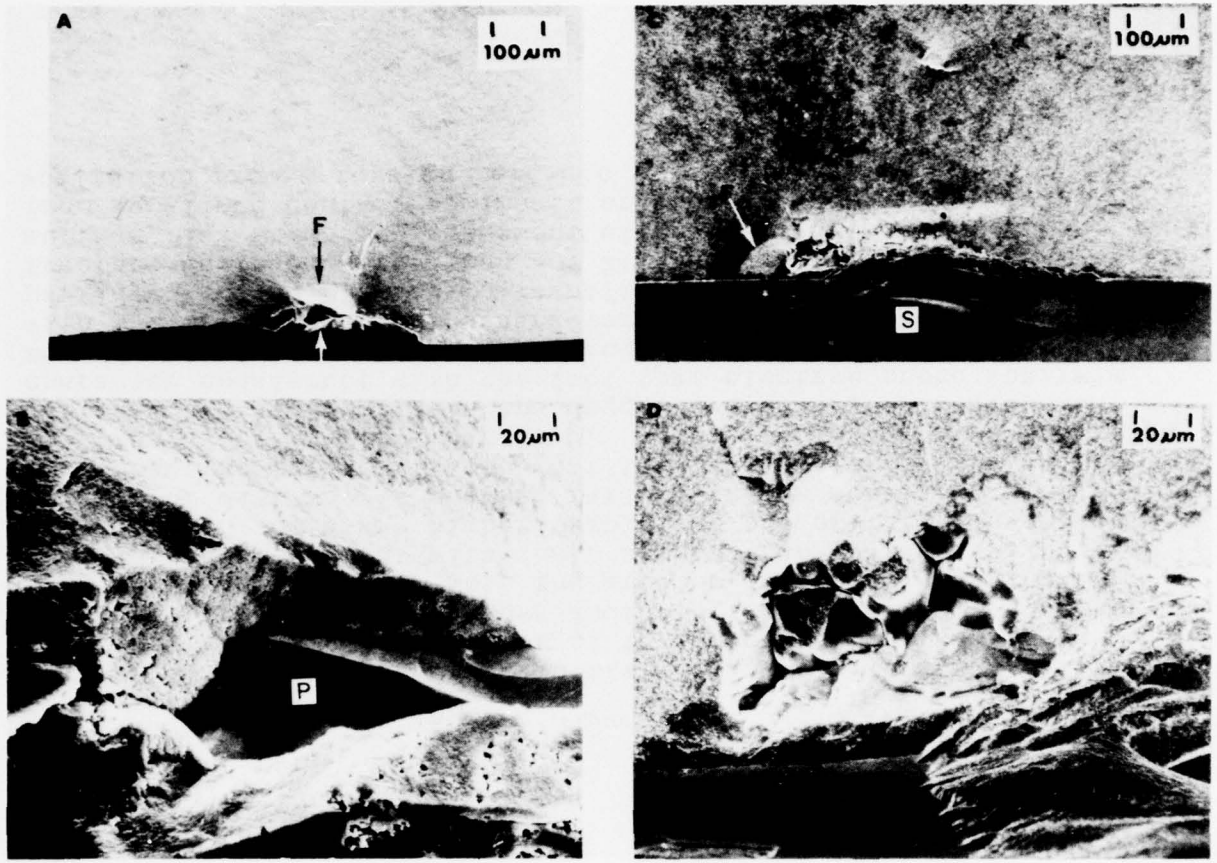
A
100 µm
F
B
100 µm
S
C
20 µm
P
D
20 µm

Figure 3

Additional examples of MgF_2 disks failing from large particles A and B are photos of the actual fracture surface of specimen No. 22 of Table 1. Note the approximately semi-circular flaw having propagated out from the foreign particle, P, which is shown in greater detail in B. Because of the only partially exposed nature of this particle and the flaw propagating out from it, this specimen was first listed as failing from a surface flaw (Table 1). This illustrates the fact that some specimens actually failing from particles were not detected to have such fracture origins by optical examination. C and D are photos of the fracture origin of specimen No. 29 of Table 1. Note a flaw propagating out from the left side of a cluster of particles, shown at higher magnification in D Electron probe analysis showed to these particles to be of essentially the same composition as the matrix, i.e. MgF_2. Note also the surface spallation (labeled S in C) which is believed to have occurred during or after failure.

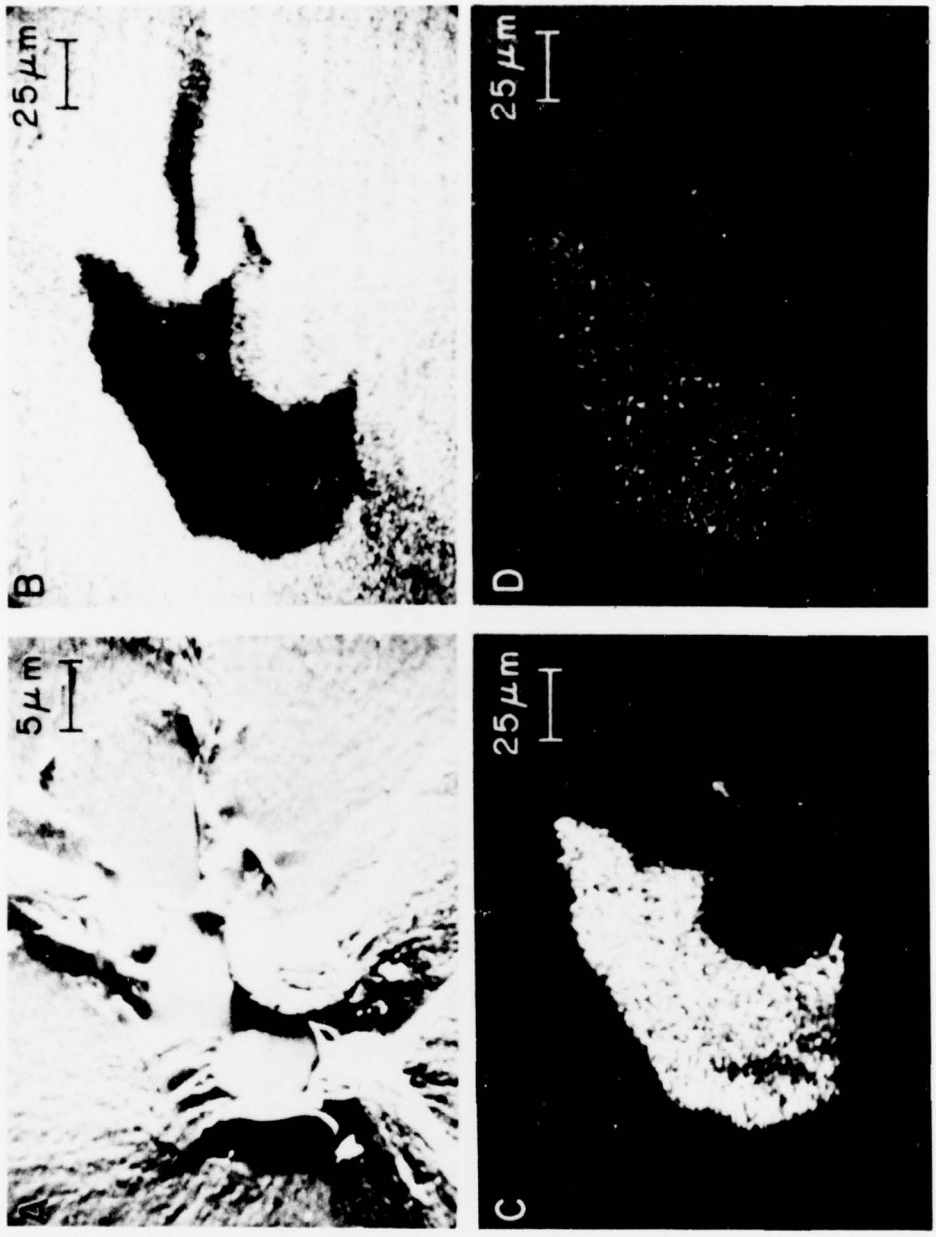
B
25 μm
D
25 μm
C
25 μm
5 μm

Figure 4

Sample electron probe analysis of foreign particle failure in MgF_2. A is an electron backscatter presentation showing a foreign particle at the fracture origin of a specimen (No. 103-2 of Table 2). B is the magnesium x-ray fluorescence showing that the particle is clearly not MgF_2 while photos C and C are respectively silicon and oxygen x-ray fluorescence showing the particle clearly consists of silicon and oxygen. The relative count rates (~ proportional to the density of white dots) are consistent with the count rates obtained off a calibration sample of pure SiO_2 in the probe. These results are typical of several analysis made in the probe.

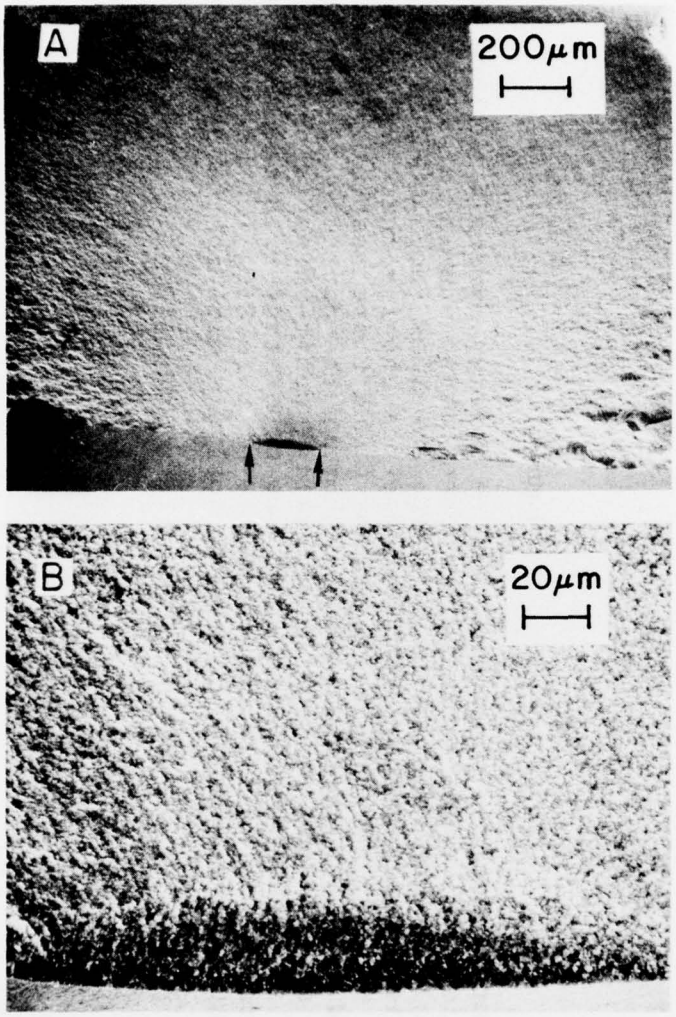
A
200μm
B
20μm

Figure 5

MgF_2 disk failing from a machining flaw. A and B are SEM photos of the actual fracture surface of specimen No. 7 of Table 1 which failed from a surface machining flaw bounded by the arrows in A and shown in higher magnification in B. The elongated shape of this flaw as well as the smooth flaw periphery suggest that this is a flaw from the final stages of finishing the disk, i.e. polishing, rather than a part of coarser flaw left over from earlier grinding.

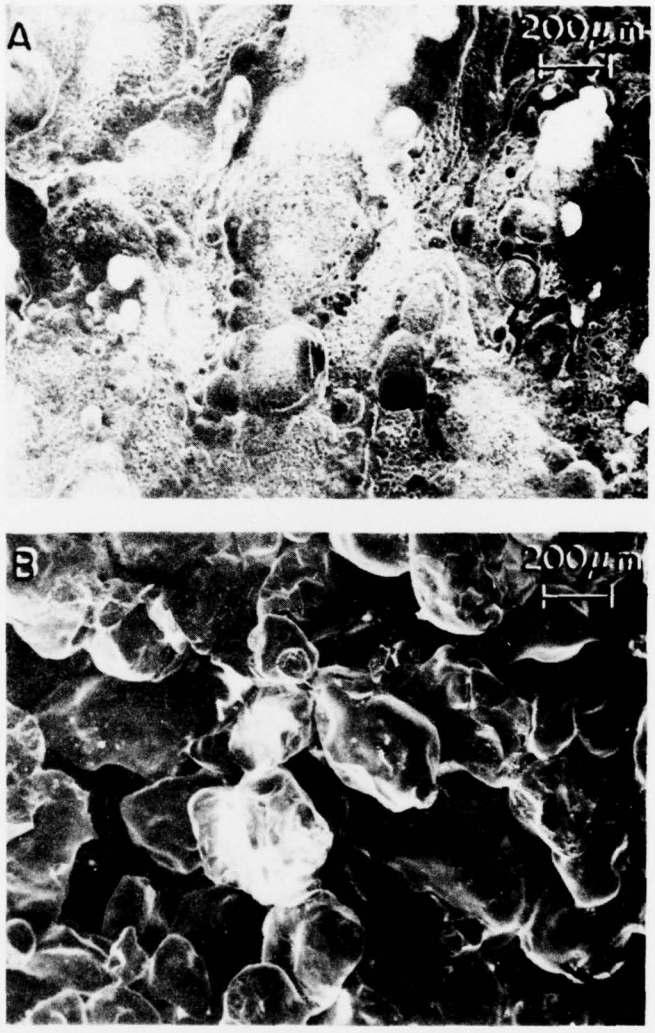
A
200 μm
B
200 μm

Figure 6

SEM photos of surfaces SiO_2 crucible used for MgF_2 powder processing.
A) Crucible interior. Note many circular depressions.
B) Crucible exterior. Note relatively loosely bonded SiO_2 grains of similar sizes to those found in the hot pressed MgF_2.

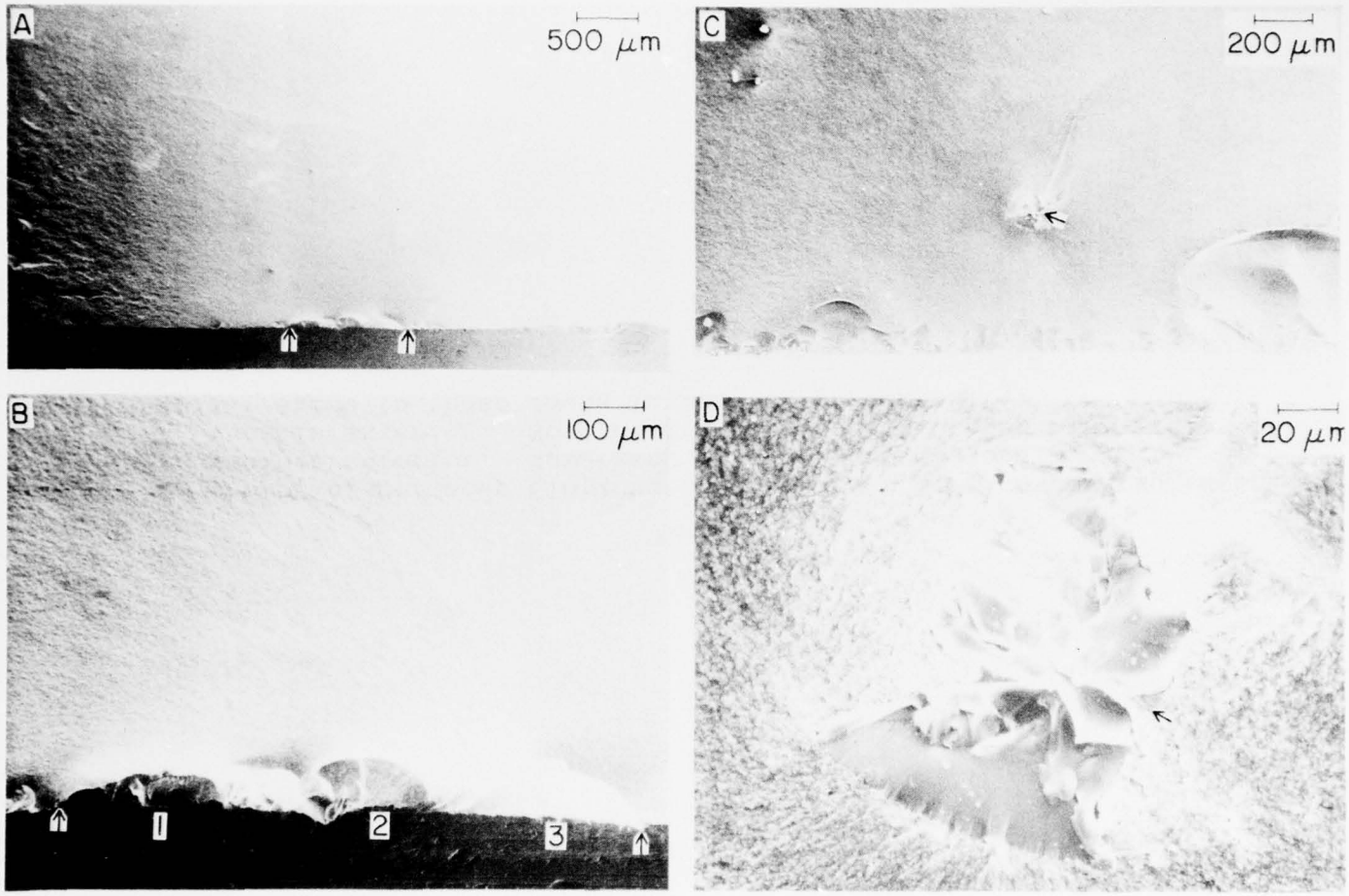
A
500 μm
C
200 μm
B
100 μm
1
2
3
D
20 μm

Figure 7

Fracture of large (0.5" x 0.75" cross section) MgF_2 bars broken in 3 point flexure (3.5" span) A and B are progressively higher magnification photos of a bar failing ($\sigma_f \sim 8.5$ ksi) from an elongated machining flaw (between arrows) from machining perpendicular to the bar axis. Note the flaw consists of at least 3 major crack segments. C and D show the fracture of a bar ($\sigma_f \sim 13.6$ ksi at the surface, ~ 12.2 ksi at particle) from 1 or 2 particles (arrows) identified by EDAX as having a strong Si, but no Mg, signal and hence assumed to be SiO_2. Note also the spalling at the intersection of the fracture and tensile surface near the bottom of C due to the intersection of the cracks propagating from the particles and cracks propagating from machining flaws.

50μm
500μm
2.6"
A
B
C
D
E

Figure 8

Failure of an actual MgF_2 Sidewinder dome. A is a low magnification photo showing the fracture pattern in a dome from a thermal shock test conducted at China Lake (dome courtesy of Dr. Frank Markarian of NWC). Failure initiated between the two pieces labeled 1 and 2, with B and D being higher magnification photos of the failure causing flaw as seen on piece No. 1 and C and E are the progressively higher magnification photos of the fracture surface showing the flaw as it is seen on the fracture surface of piece No. 2. Since the flaw is not as clear in E, its approximate periphery has been outlined by arrows. Note that the somewhat different appearance of the flaw in these two matching halves of the fracture surface is due to some variation in the orientation of the two fracture halves in the SEM. These show excellent agreement between one another considering the orientation differences. The fracture stress calculated independently from both the flaw size and the mirror size observed each gave approximately 10,000 psi which is in good agreement with the expected failure stress from analytical predictions made at NWC (private communication, Dr. Frank Markarian). Note also that the failure causing flaw was on the inside of the dome consistent with the analytical expectations. The character of this flaw is highly suggestive on one from machining, most likely the final polishing operation.